

# Significance of Channel Planform Change and Morphometric Indices in the Buri River Basin, India and Bangladesh



Saheli Bhattacharjee, Sunando Bandyopadhyay, and Sunil Kumar De

**Abstract** The Indian state of Tripura and the adjacent parts of eastern Bangladesh are characterised by six N–S aligned westerly arcuate anticlinal ridges of the Chitragong–Tripura Fold Belt (CTFB), uplifted during the Pleistocene. The Buri (107 km in 2017) originates from the western flank of the CTFB’s Baramura Range (247 m) and drains into the Meghna system of the Ganga–Brahmaputra–Meghna Delta. Maps and images of 1931–34 (Survey of India ‘inch’ maps), 1962 (Corona photos), 1975 (Landsat-1 MSS image), and 2017 (Resourcesat-2 L4-fmx image) show that the river markedly changed its planform during the last 84.5 years. Based on valley directions and characteristics, the Buri is divided into 37 reaches. Of these, sinuosity indices (SI) of 36 are calculated for the four survey/imaging years to determine the extent of change. Shuttle Radar Topography Mission elevation data (3 arc second tiles) of the region are utilised to bring out structural signature on drainage using profile shape, normalised stream length-gradient (SLk) index, and basin asymmetry factor (AF).  $\chi$ -map of the Buri and its surrounding basins is taken into consideration to observe the topographic stability of this region. Finally, long-term rainfall records close to the Buri Basin (932 km<sup>2</sup>) are analysed as proxies for change in discharge. The results show that the Buri is antecedent to all anticlinal axes along its course. Overall, its 1931–34—2017 SI decreased in 64% of the reaches (1.58–2.76 to 1.02–1.17). Within the hills, increase in 1931–34—2017 channel SI coincided with high SLk values (>2) as well as profile convexity in two stretches, suggesting neotectonic uplift. In two other convexity zones, the 1931–34—2017 SI decreased contradictorily, possibly due to local aggradation or modification. An AF of 31 indicates that the Buri Basin has a probable tilt to the north. The  $\chi$ -map of the area shows that the water divide is migrating towards the basin at its headwater region. Any statistically significant change in long-term rainfall records close to the basin is not present. Landuse alterations in the basin is also small, and unlikely to impact planform changes. In its deltaic stretch, the reasons for drastic change in the Buri’s sinuosity index (1.40–4.13

---

S. Bhattacharjee · S. Bandyopadhyay (✉)  
Department of Geography, University of Calcutta, Kolkata 700019, India  
e-mail: [sunando@live.com](mailto:sunando@live.com)

S. K. De  
Department of Geography, North Eastern Hill University, Shillong 793022, India

to 1.08–1.26) can principally be ascribed to channelisation that reduced its length by 55% between 1931–34 and 1962; sinuosity of the river is slowly increasing thereafter.

## 1 Introduction

Among the geomorphic elements of a landscape, river networks are most sensitive to any change in the existing balance between tectonics, climate, and catchment area landuse. In an unstable region, changes in planform of a river are often caused by spurts in subtle tectonic or isostatic activity. Therefore, progressive alterations in channel planforms are widely used as reliable indicators of orogenic or epeirogenic movements in many parts of the world (Seeber and Gornitz 1983; Ouchi 1985; Burbank and Anderson 2012). River planform changes can also be induced by variations in water and sediment discharge due to changes in climatic forcings or landuse characteristics in the basin (Kiss and Blanka 2012); or by a combination of all these factors (Goudie and Viles 2010). Besides channel planform changes, morphotectonic indices, derived from basin elevation and channel gradient characteristics, are commonly used for detecting active deformations, even in a region with a low rate of tectonic activity (Pedrera et al. 2009; Ntokos et al. 2016).

‘Neotectonics’ refers to the study of crustal movements that occurred in the geologically recent past and that may be ongoing today (Stewart 2004). The term ‘Neotectonics’, emerged from the papers of Obruchev in 1936 and 1948, used to denote crustal structures created during the Neogene. It currently purviews to ‘fully explain all the characteristics of the contemporary relief of the land surface of the entire globe’ (Beckinsale and Chorley 1991:171, Chandra 2012).

This article traces the changes in the planform of the Buri, a sixth order stream of the western Chittagong–Tripura Fold Belt (CTFB) during 1931–34—2017 and analyses selected morphometric indices to assess the nature of neotectonic and climatic imprints on the river. Although some previous works exist on tectonic geomorphology on some parts of the CTFB (Bandyopadhyay and De 2009; Dey et al. 2009; De and Bandyopadhyay 2011; Bandyopadhyay et al. 2013; Valdiya and Sanwal 2017), the Buri has been taken up for study for the first time.

## 2 Study Area

### 2.1 Location

The 107-km Buri drains some 932 km<sup>2</sup> between 90°57′–91°35′ E and 23°28′–57′ N. It emanates from the 247-m Baramura Range at an altitude of ~200 m, takes up a general west-southwestward course for its first 72 km (2017 length) up to its debouchment into the deltaic plains through the Rakhia Range at Nayanpur. In this section, the

Buri's course is marked by confined passages towards the source, gradually giving way to broad intervening alluvial and colluvial valleys below 70 m. Bishalgarh, an important town of the Indian state of Tripura (Sepahijala District), is located in this section. As the river enters the Ganga–Brahmaputra–Meghna Delta (GBMD) plains at 10 m, it crosses over into the Bangladeshi district of Comilla and takes up a northwestward course of 35 km up to its outfall into a partially cut-off meander of the Pagla (lower Titas), a spill channel of the Meghna, near Nabinagar (Fig. 1). The course of this cut-off, upstream of its confluence with the Buri, largely degenerated during 1931–34—1962. Its lower part is now maintained by the discharge from the latter. This effectively increased the length of the Buri by 4.6 km. The final 22 km of its course between Kuti and the outfall used to be tidal in 1931–34. Stretches of the Buri is also known as the Bijai in Tripura and the Saida in Bangladesh.

## 2.2 Geology

After India separated from the eastern Gondwanaland and started to drift north in the early Cretaceous (Lawver et al. 1985), the Indian plate started an oblique and rotational subduction beneath the Burmese microplate that formed the Indo-Burman Ranges (IBR) in the Cenozoic. The remnant ocean basin at the western edge of the Burmese plate was subjected to a 'zipper-like' closure from north to south (Biswas and Agrawal 1992; Steckler et al. 2016). The sediments eroded from the Barail and Naga Hills on the north and the IBR on the east formed an accretionary prism in its arc-trench setting and eventually got folded, faulted, and uplifted in form of the CTFB, mostly during the Pleistocene (Nandy 2001; Maurin and Rangin 2009) (Fig. 2). From west to east, this fold belt is comprised of six major westerly convex anticlinal ridges of increasing altitude and age of deformation—Rakhia, Baramura, Atharamura, Longtarai, Machhlithum and Jampui—separated by the synclinal valleys of Agartala, Khowai, Dhalai, Manu, and Juri–Deo, respectively (Fig. 1b). On its western edge, the Buri flows across the structural grain of the CTFB.

The CTFB is mainly characterised by repetitive successions of fine- and coarse-grained poorly consolidated flysch sediments of four discernible formations belonging to Miocene–Pleistocene with Quaternary alluvial and colluvial deposits in the valleys (Fig. 3). Most anticlines have older formations exposed along their crests (Alam et al. 1990; Nandy 2001; GSI 2011). Sedimentation and tectonic activity of the area initiated from the east and gradually migrated towards the west. Consequently, the intensity of folding and structural complexities also decreases westward, and finally disappears under the alluvial silts and clays of the deltaic plains (Maurin and Rangin 2009; Wang et al. 2014).

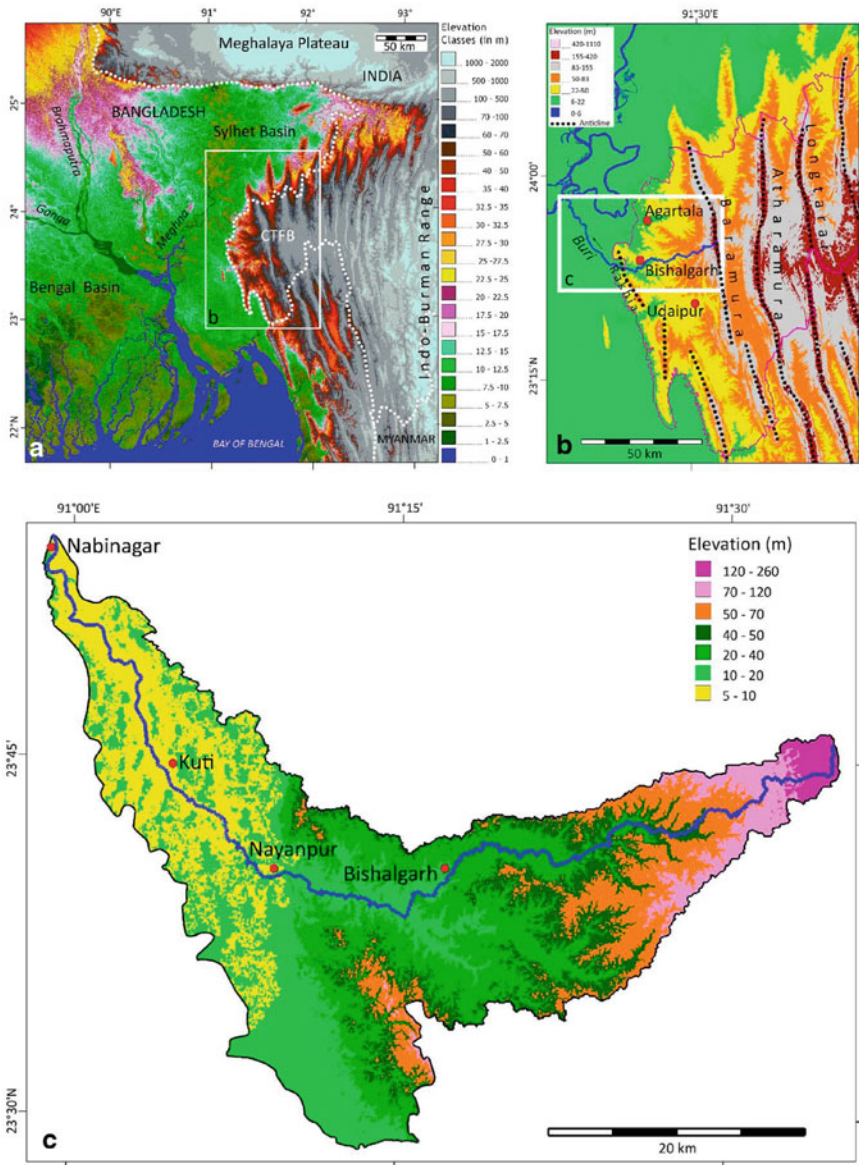


**Fig. 1** Physiographic setting of the Buri basin. **a** Chittagong–Tripura Fold Belt (CTFB) located at the eastern margin of the Ganga–Brahmaputra–Meghna Delta. **b** The principal anticlinal ridges forming the northern portion of CTFB. **(c)** The course of the Buri and elevation distribution in its basin. Scales of the maps increase clockwise from upper left; positions of enlarged area shown by white rectangles. *Source* Based on SRTM 3 arc second data of 2000

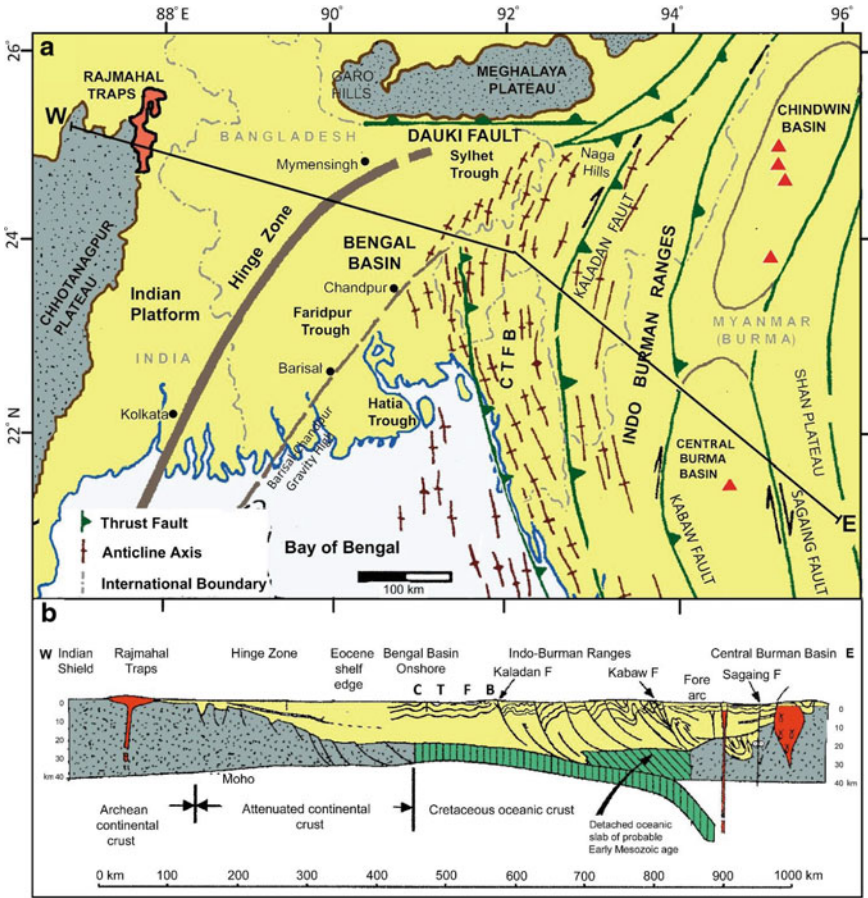


**Fig. 2** Tectonic setting of the Chittagong–Tripura Fold Belt (CTFB). **a** Major tectonic and geological features of the Bengal Basin and its surrounding highlands. The Hinge Zone represents the edge of the continental shelf of India. The Barisal-Chandpur Gravity High (BCGH) indicates the transition between the continental and oceanic crusts of the subducting Indian plate. Red triangles denote tertiary volcanic centres. **b** Schematic W–E cross section shows the CTFB region as folded and uplifted sedimentaries formed at the arc-trench location. *Source* Based on Alam et al. (2003). Some elements are incorporated from Nandy (2001), Gani and Alam (2003), and Bandyopadhyay (2007)

### 3 Materials and Methods

#### 3.1 Maps and Images: Availability

To study the planform change of the Buri, four datasets spanning 84.5 yr have been considered with an average interval of 28 yr. The details of these are shown in



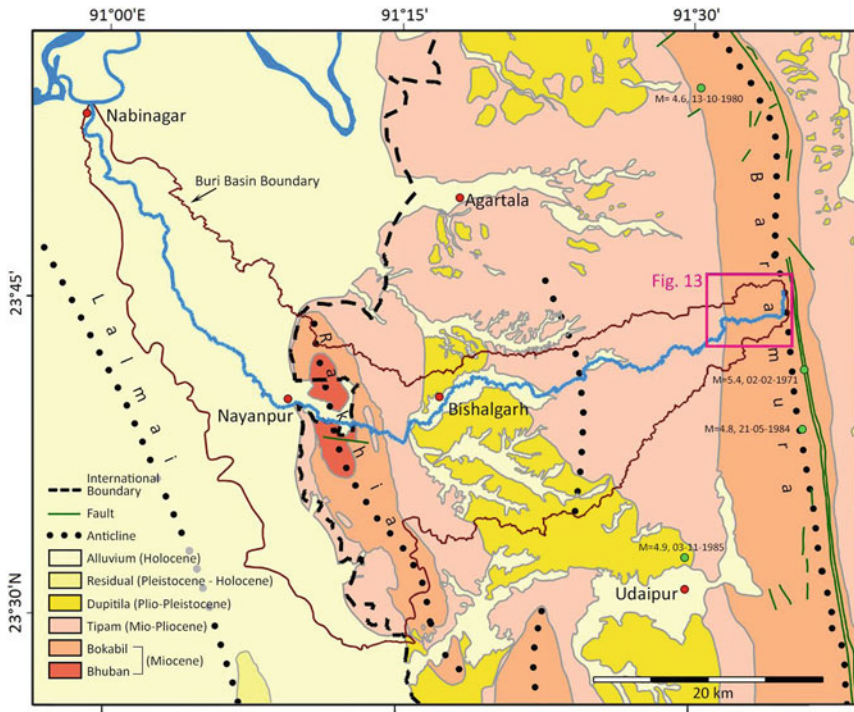


**Fig. 3** Geology of the Buri basin and its surrounding area. *Source* Compiled from Alam et al. (1990), Persits et al. (2001), GSI (2011), Wang et al. (2014)

Table 1. Besides these, vector  $\chi$  (chi) maps of the Buri and its surrounding basins, were retrieved from <https://www.nature.com/articles/sdata2018127> (Giachetta and Willett 2018).

### 3.2 Maps and Images: Processing and Digitisation

The six Survey of India ‘one inch’ toposheets surveyed in 1931–34 were individually georeferenced using graticule intersections and mosaiced to a file pertaining to Everest spheroid and Universal Transverse Mercator (UTM, zone 46-Q) projection. The available 1974–75 Survey of India ‘metric’ toposheet was similarly rectified. The MSS scene was georeferenced at source and the LISS-4 scenes were obtained as precision orthorectified products on WGS-84 spheroid and UTM projection. These were reprojected to Everest datum and mosaiced where necessary. The three Corona space-photos were orthorectified and mosaiced on the basis of the georectified LISS-4 fmx mosaic. Finally, the SRTM 90-m (3 arc second) elevation data, available on WGS-84, were reprojected to match the referencing of the other maps and images.

**Table 1** Maps and images used in the study

Data type <sup>a</sup>	Source <sup>a</sup>	Particulars	Year of survey/date of pass	Resolution/scale
Survey of India 'one-inch' topographical maps	–	Six maps: 79I/13, 79 M/01, 02, 06, 09, 10	1931–34	1:63,360
Corona Photos	USGS: <a href="https://earthexplorer.usgs.gov">https://earthexplorer.usgs.gov</a>	Three scenes: DS009048070DF268_b, DS009048070DF269_b, DS009048070DF267_b	1962-Nov-24	~2 m
Survey of India 'metric' topographical map	–	One map: 79 M/09	1974–75	1:50,000
Landsat-1 MSS Image	USGS: <a href="https://glovis.usgs.gov">https://glovis.usgs.gov</a>	One scene: Path-147, Row-43	1975-Mar-27	60 m
Resourcesat-2 LISS-4 fmx Images	NRSC: <a href="https://uops.nrsc.gov.in">https://uops.nrsc.gov.in</a>	Two scenes: Path-110, Row-55, Subscenes-B, -D	2017-Feb-12	5 m (resampled at source)
SRTM elevation data	USGS: <a href="https://glovis.usgs.gov">https://glovis.usgs.gov</a>	Two tiles: n23e90, n23e91	2000-Feb	90 m (3 arc-second)

*Note* <sup>a</sup>fmx: full scene multi-spectral; LISS: Linear Imaging Self Scanner; MSS: Multi Spectral Scanner; NRSC: National Remote Sensing Centre; SRTM: Shuttle Radar Topography Mission; USGS: United States Geological Survey

It requires to be mentioned here that elevation models of finer resolutions could not be used for the Buri Basin due to several data inconsistencies.

The course of the Buri was digitised from the four datasets of 1931–34, 1962, 1975, and 2017 following the mid-line between riverbanks as channel mid-lines remain mostly unchanged even during floods (Friend and Sinha 1993). The 1974–75 Survey of India 'metric' topographical map covered only a part of the Buri Channel and was referred to as supplementary data of the 1975 MSS image.

The 2000 SRTM elevation data were utilised to bring out morphometric heterogeneity of the basin by bringing out the Buri's basin boundary, long profile shape, normalised stream length-gradient (SLk) index, and basin asymmetry factor (AF).

All georeferencing, mosaicing, and digitisation of the maps and images were carried out using Geomatica v2015 software. ArcGIS v10.3.1 was used for extraction of morphometric parameters from the elevation model. Presentation of all statistical data was done through Microsoft Excel v365.

### **3.3 Extraction of Morphometric Indices**

#### **3.3.1 Basin Boundary Extraction**

The Buri's basin boundary was auto-extracted from the 2000 elevation data. Minor adjustments of the perimeter were done to preserve compatibility to drainage configuration close to its outfall locality.

#### **3.3.2 Channel Reach Demarcation**

Based on the breaks in the Buri's valley directions and adjacent topography, its course was divided into 37 reaches (Fig. 5). Among these, Reaches 1–4 represent the Buri's flow through the Baramura Hills, Reaches 5–28 through confined valleys, and Reaches 29–36 through the GBMD plains. The lowermost section of the Buri that got extended due to degeneration of the upper Pagla (see Sect. 2) was considered as Reach 37. This reach was not included in the comparative study of sinuosity indices.

#### **3.3.3 Sinuosity Index**

Sinuosity index is used for determining the degree of curvature of a channel. This work followed the relationship proposed by Schumm (1963):

$$\text{Sinuosity Index (SI)} = \text{Channel Length/Valley Length}$$

The channel length is measured along the midline of the riverbanks between two selected points and the valley length is the straight-line distance between the same two points. SIs were calculated for Reaches 1–36 for the four mapping years (Fig. 5). Changes in reach-specific values of SI obtained for these four years are shown in Fig. 6.

#### **3.3.4 Profile Analysis**

The long profile of the Buri was computed on the basis of its 2017 course and 2000 elevation data. The extracted profile line was smoothened by running 80-pixel ( $\cong 7.2$  km) moving average. This is represented in Fig. 7, with the zones of convexity indicated in it.



### 3.3.5 Normalised Stream Length–Gradient Index

Stream Length–Gradient Index (SL) is used for identifying surface signature of tectonic activity and geology of a region. Hack (1973) proposed Stream Length–Gradient Index (SL) for a channel reach using the relationship:

$$SL = \frac{\Delta H \times L}{\Delta L}$$

where,  $\Delta H$  is the change in elevation of the reach,  $L$  is the total channel length from the midpoint of the reach to the highest point on the channel, and  $\Delta L$  is the length of the reach.  $\Delta H/\Delta L$  is the reach slope or gradient.

However, SL Index, per se, often proves inappropriate for comparing rivers of different lengths, as its value depends on river length. Therefore, to normalise the SL index, the SL value of each reach is divided by the gradient index of the entire river profile ( $k$ ), which returns more reliable results for identifying long profile anomalies (Seeber and Gornitz 1983; Pérez-Peña et al. 2009; McCleary et al. 2011). McCleary et al. (2011) used the following expression to determine  $k$ :

$$k = (h_s - h_f)/\ln(L_t)$$

where,  $h_s$  denotes the river head elevation,  $h_f$  is the elevation of the river mouth,  $\ln$  is natural logarithm, and  $L_t$  is the total length of the river. The values of normalised stream length–gradient index (SL $k$ ) are positively correlated with steepness of channel profiles. The SL $k$  indices of the 37 reaches of the Buri were derived using its 2017 planform and 2000 elevation data.

### 3.3.6 Asymmetry Factor

Asymmetry Factor (AF) is used for determining topographic tilt of a drainage basin in order to understand its tectonic deformation (Hare and Gardner 1985). It uses the following formula:

$$AF = (A_r/A_t) \times 100$$

where,  $A_r$  is the drainage area right of the main channel facing downstream, and  $A_t$  is the total area of the drainage basin.

If AF is >50%, the channel is positioned close to the left divide of the drainage basin, length of the tributaries are usually longer in the right side of the basin than on the left, and the basin is left-tilted; AF < 50% reverses these observations. AF = 50% indicates little or no tilting perpendicular to the direction of the master stream (Keller and Pinter 2002). AF values vary significantly under the effects of tectonic renewal

or strong lithologic control (Ntokos et al. 2016). To obtain AF of the Buri, its basin boundary extracted from the 2000 elevation data and the 2017 channel configuration were used.

### 3.3.7 Chi Index

Willett et al. (2014) proposed the idea of landscape equilibrium through divide migration among drainage basins. The quantity  $\chi$  (chi) is calculated from digital elevation data and it provides a measure of the length of a channel or the height of a point in the channel, normalised for basin area. In a tectonically active region having similar physical property, divides of a drainage basin having lower value of  $\chi$  tends to move towards the drainage basin with larger  $\chi$  value to reach equilibrium. The  $\chi$  values of the Buri and its adjacent channel networks were retrieved from <https://www.nature.com/articles/sdata2018127#ref-CR33> (Giachetta and Willett 2018).

## 3.4 Analysis of Rainfall Trends

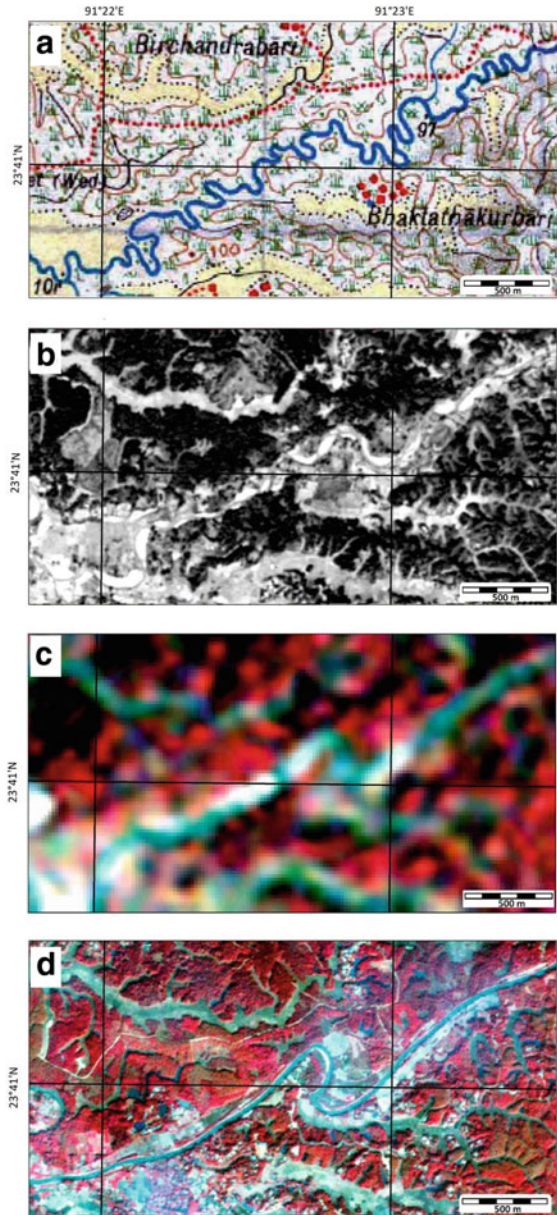
Annual rainfall records of the two nearest India Meteorological Department stations of the Buri Basin, at Agartala (14 km from basin, on the north) and Udaipur (15 km, on the south) were obtained for 1953–2013 (61 yr,  $n = 56$ ) and 1938–2003 (66 yr,  $n = 64$ ), respectively. These data were trend analysed to get some idea on long-term discharge variation of the Buri, because any information on discharge of the river was unobtainable.

## 4 Results

The results obtained from the analyses of the maps, images, elevation, and climatic data are presented in Figs. 4, 5, 6, 7, 8, 9, 10, 11, and Table 2.

Between 1931–34 and 2017 (84.5 yr), the Buri tended to shorten course by lowering its sinuosity in 25 out of 36 reaches (Figs. 5 and 6). E.g., in Reach 17 between Nabachandrabari and Gholaghati, its length decreased from 9.45 km to 5.64 km and sinuosity from 2.1 (meandering) to 1.2 (sinuous). In Reach 20 between Sipahijala and Kasba, length of the river reduced from 4.46 km to 3.09 km and sinuosity from 2.0 (meandering) to 1.3 (sinuous). In Reach 33 near Kutí, the channel shortened from 8.48 km to 4.37 km and the sinuosity from 2.15 (meandering) to 1.09 (straight). The shortening was most pronounced in its lower stretch over the GBMD plains. Increase in sinuosity, on the other hand, was detected near the source (Reaches 1–8) and in the mid-section (Reaches 23–25). Overall, the river decreased its length by 30.4% from 154 km (1931–34) to 107 km (2017). If looked into the interim imaging years of 1962 and 1975, sinuosity changes altered direction in a

**Fig. 4** Changes in the Buri river sinuosity in Reach 17, represent the databases used in the study. Planforms in **a** 1931–34, **b** 1962, **c** 1975, and **d** 2017. Composite planform of all years and position of Reach 17 are shown in Fig. 5. *Source* See Table 1



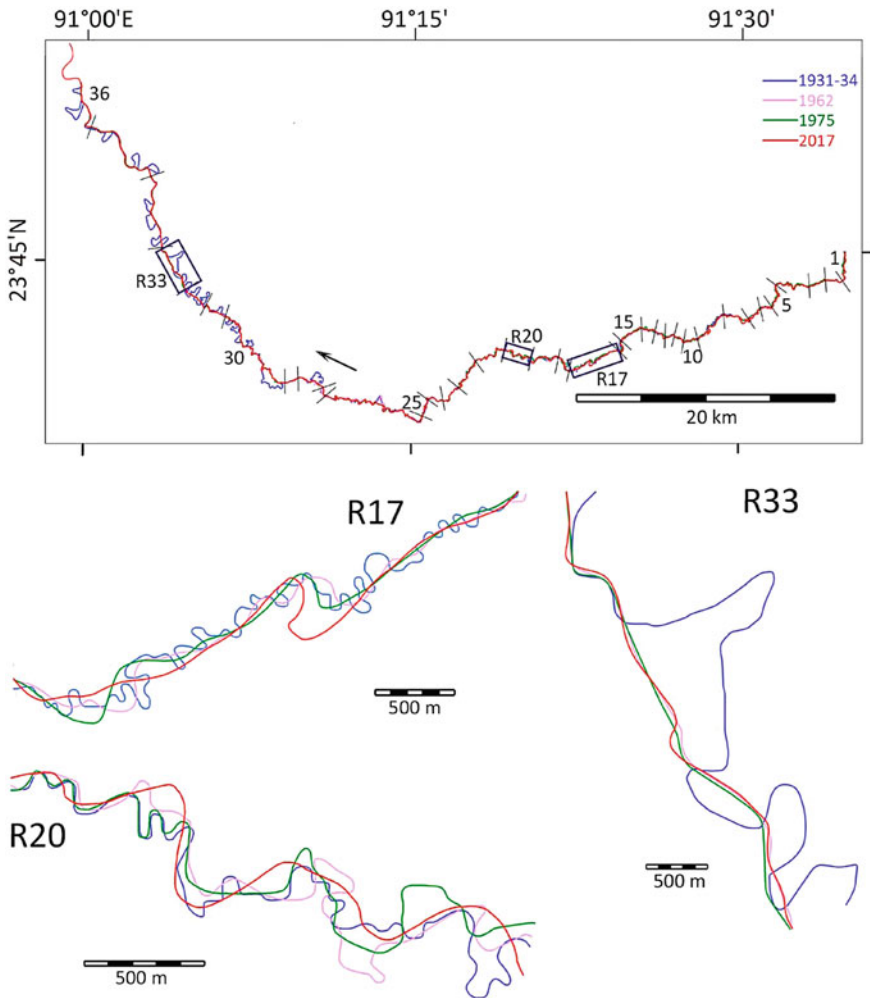


**Fig. 5** Changes in the Buri river sinuosity from 1931–34 to 2017. ‘R’ stands for Reach. Numbers indicate Reach IDs. Details of Reaches 17, 20, and 33, indicated by black rectangles in the Buri’s course, are enlarged in the lower part of the diagram. Note the differences in scale in all four maps. *Source* see Table 1

number of sections; most notably in Reaches 5, 7–9, 11, 15, and 18 in the hills and in Reaches 19, 21, 23, and 27 in the plains. In the Buri’s lowermost stretch (Reaches 31–36), although drastic reduction in sinuosity, reducing up to 75% of reach lengths, was recorded between 1931–34 and 1962, slow and continuous rise in sinuosity was seen between 1962 and 2017. The 2017 reach-specific SI of the Buri, classified into very low (SI: < 1.05), low (1.05–1.25), medium (1.25–1.5), and high (>1.5), are shown in Fig. 8.

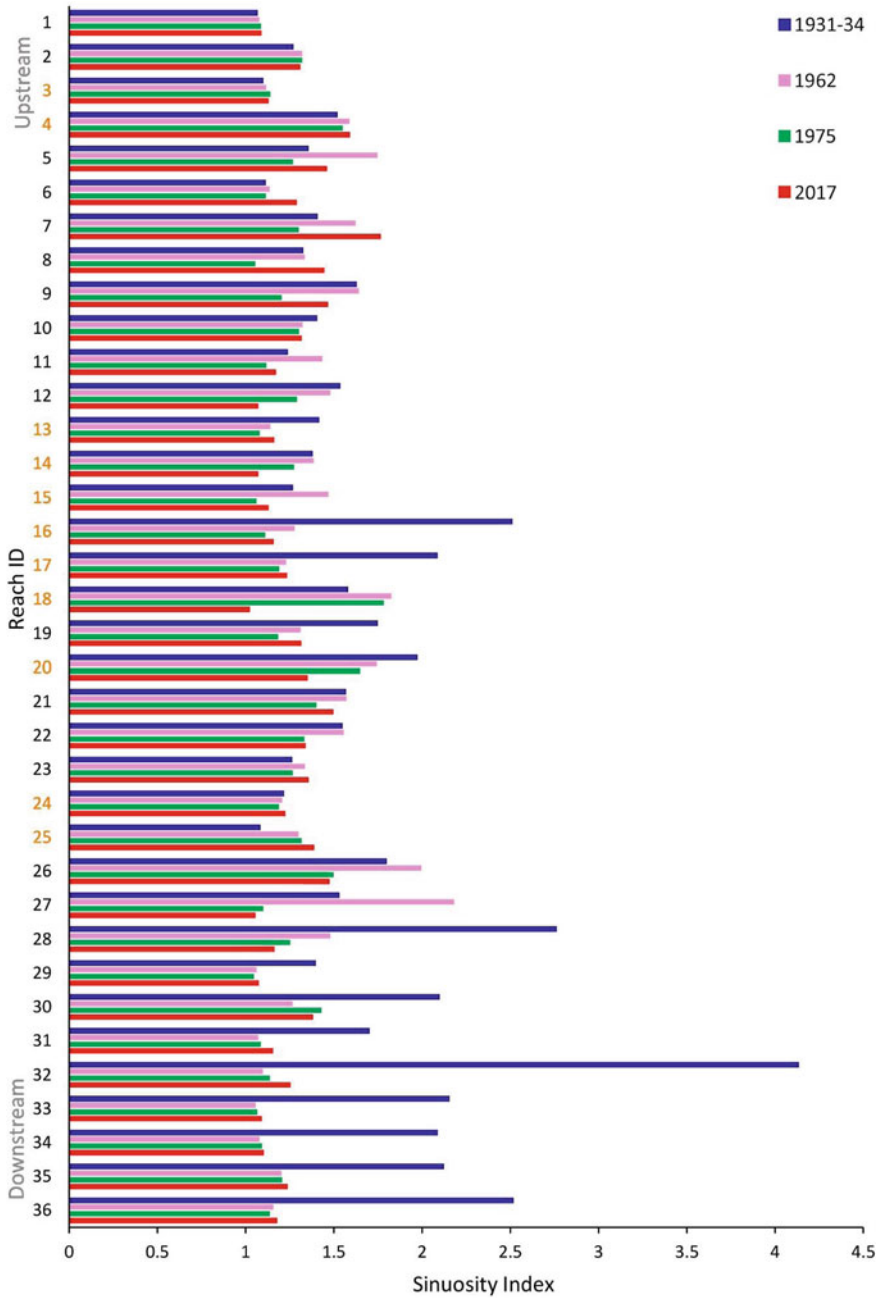


**Fig. 6** Reach-specific sinuosity index values of the Buri between 1931–34 and 2017. Reach IDs falling in the four convexity zones of channel profiles are shown in orange. *Source* see Table 1

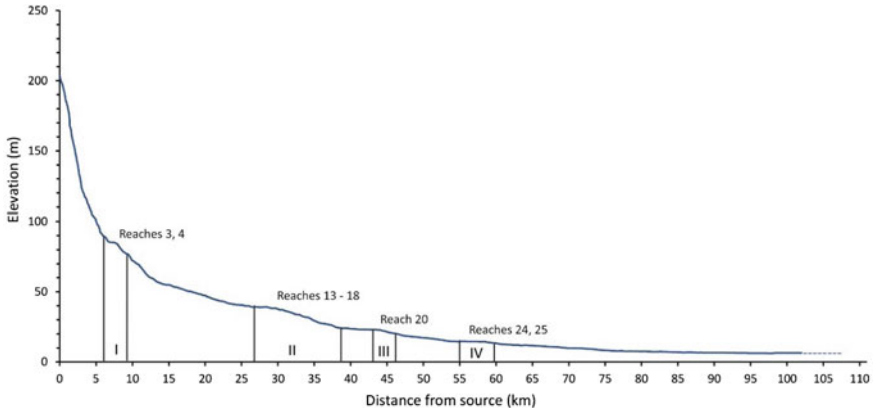


**Fig. 7** Long profile of the Buri River. Zones I–IV represent profile convexity that may indicate presence of uplift. *Source* Based on SRTM data of 2000 and Resourcesat-2 LISS-4 fmx data of 2017. See Table 1 for details

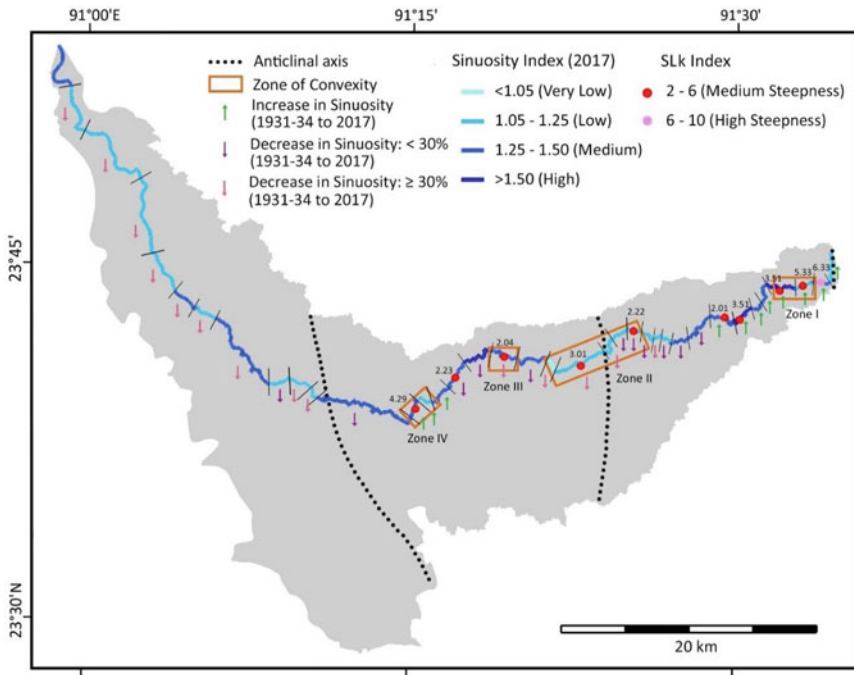


**Fig. 8** Composite map of the Buri showing the four profile convexity zones, 2017 reach-specific sinuosity index ranges, SLk indices representing medium to high steepness, and known anticlinal axes. Trends of 1931–34—2017 change in sinuosity indices are shown by vertical arrows. Reach adjacent numbers indicate SLk index values. See text for further explanation. See Fig. 5 for reach IDs



Along the Buri’s long profile, four zones of convexity were detected that are represented by Reaches 3 & 4, 13–18, 20, and 24 & 25 (Fig. 7). Reach-specific SLk indices, as derived from the Buri’s profile analysis can be classified into the groups of <2 (low steepness), 2–6 (medium steepness), and 6–10 (high steepness). Table 2 summarises the main characteristics of the Buri’s reach-wise sinuosity with salient features of its profile convexity and SLk indices. Figure 8 spatially overlays these attributes over the Buri’s 2017 SI and trends of 1931–34—2017 SI change.

AF of the Buri Basin was found to be 31.02 (Fig. 9), which denotes that it is asymmetric and tilted towards the right (north).

Classification of the drainage networks of the Buri and its surrounding basins according to their  $\chi$  values showed marked discrepancy between the headwaters of the Buri and the streams of the Khowai basin on their opposite side (Fig. 10). The higher values of the Buri (18.59–20.02) compared to the Khowai basin (12.37–14.30) designate the former as the ‘victim’ and the latter as the ‘aggressor’. This denotes that the drainage divide between the two basins is shifting westwards along the crest of the Baramura Range, towards the Buri’s direction.

Finally, long-term rainfall records of the Buri Basin region (Fig. 11) showed average decrease of 3.2 mm/yr towards the north of the basin (Agartala) and average

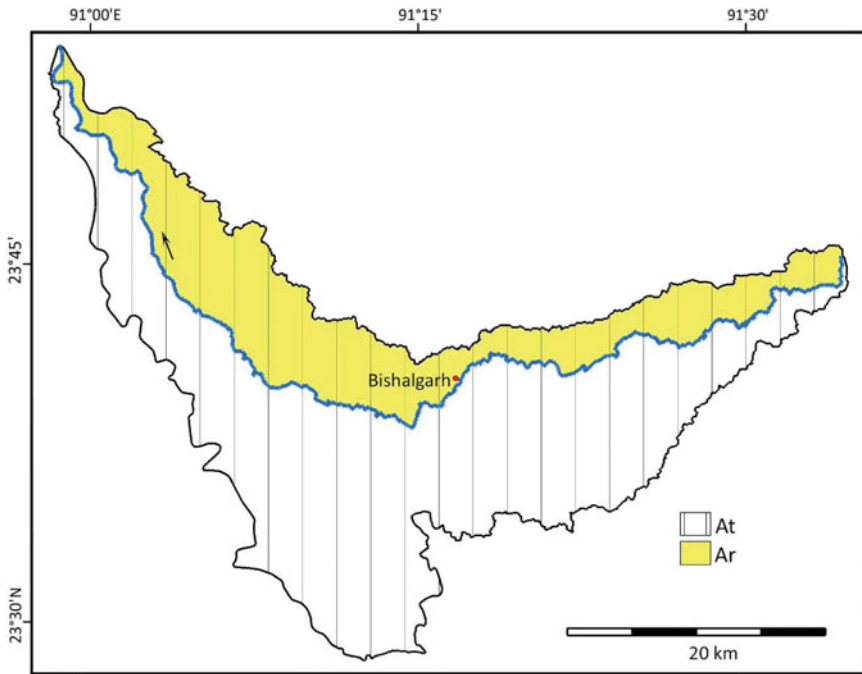


**Fig. 9** Topographic asymmetry of the Buri Basin. ‘At’ and ‘Ar’ stand for total basin area and area of the basin to the right of the main channel facing downstream, respectively. *Source* Based on SRTM data of 2000 and Resourcesat-2 LISS-4 fmx data of 2017

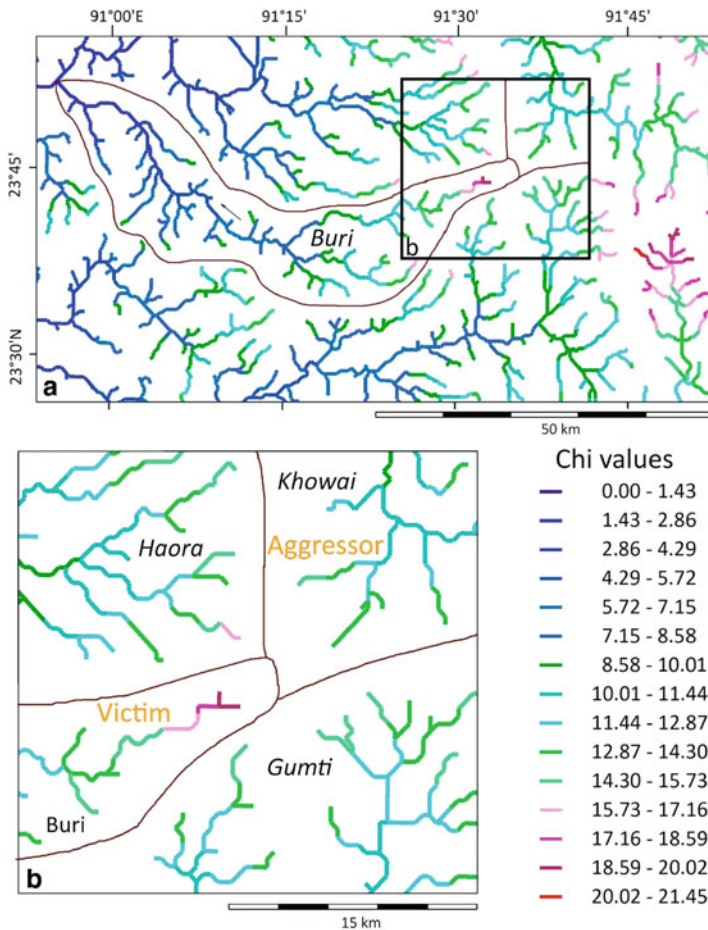


**Fig. 10**  $\chi$  values of Buri and its surrounding basin. See text for explanation. *Source* Data from <https://www.nature.com/articles/sdata2018127#ref-CR33>

increase of 6.2 mm/yr towards the south (Udaipur). Both trends, however, are statistically insignificant, but at  $p = 0.053$ , the trend for Udaipur is barely so. If these trends are projected to the timespan of data availability, the regions adjacent to northern and southern boundaries of the Buri basin register a net decrease of 187 mm (8.9% of average annual rainfall of 2102 mm) and net increase of 400 mm of rains (19.2% of average annual rainfall of 2080 mm), respectively.

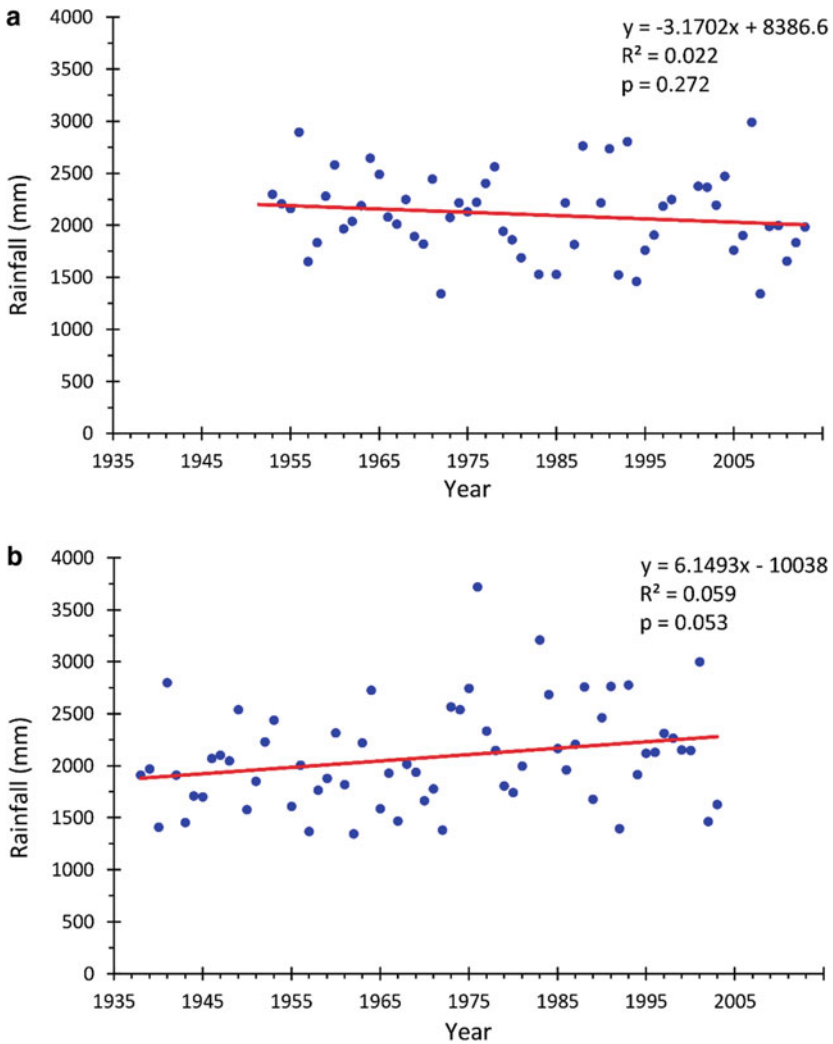


**Fig. 11** Rainfall trends of **a** Agartala and **b** Udaipur from 1953–2013 (61 yr,  $n = 56$ ) and 1938–2003 (66 yr,  $n = 64$ ) respectively. *Source* India Meteorological Department

## 5 Discussion

Decrease in sinuosity of a channel is usually caused by reduction in its slope and discharge of water and sediments—acting separately or in unison (Knighton 1998; Holbrook and Schumm 1999). These, in turn, are regulated by tectonics, precipitation and land use transformation. Tectonic change of an area can be gradual as well as episodic, effected by earthquakes. In terrains with high relative relief, earthquakes also cause landslides that augment sediment loads of the channels.

**Table 2** Morphometric parameters of the Buri: Reach-specific characteristics

Reach Id <sup>a</sup>	Overall change in sinuosity: 1931–34—2017	Long profile convexity zones	Reaches with medium and high steepness
1–4	Slight increase	Zone I: Reaches 3, 4	Reaches 2, 3, 4
5–8	General increase with decrease between 1962 and 1974–1975	–	Reaches 7, 8
9–22	Overall decrease in sinuosity, with increase in some stretches during 1931–34—1975, and 1962–2017	Zone II: Reaches 13–18, Zone III: Reach 20	Reaches 14, 17, 20, 22
23–25	Increase	Zone IV: Reaches 24, 25	Reach 25
26–28	Decrease	–	–
29–36	Major decrease between 1931–34 and 1962, followed by increase	–	–

Note <sup>a</sup>See Fig. 5 for position of the reaches

Short-term vertical subsidence and uplift rates of the CTFB synclines and anticlines measured at six places during 2003/2007–2013 using Global Positioning System (Fig. 12) indicate that these rates vary between (–) 4 mm/yr and (+) 6 mm/yr (Reitz et al. 2015). Such high rates would have considerable influence on the rivers of the region. Earthquake records from the vicinity of the Buri Basin (GSI 2011) show occurrence of four events with magnitudes 4.6–5.4 between 1971 and 1985 (Fig. 3). The events within this magnitude range only cause minor damage, and can hardly have any direct or indirect impact on channel modification. There is no record of any other notable earthquake from the region during 1931–34—2017 or some years preceding 1931–34.

An ideal graded river produces a smooth, concave-upward curve without any irregularities (Morisawa 1968). Conversely, a river profile having convexities indicates topographic anomaly that generally suggests locations of neotectonic uplift, which decreases rate of channel downcutting in absolute terms. Because channel gradient and sinuosity are positively correlated, decrease in SI occurs on the upstream side of the uplift and increase on the downstream side (Ouchi 1985).

As shown in Figs. 1 and 3, the Buri flows transverse to the structural grain of the CTFB and its path is associated with three active anticlinal axes. The river originates at the Baramura anticline, crosses another minor anticline at the central part of its upland course and breaks through the Rakhia anticline into the GBMD plains. The reach-specific 2017 SI values, direction of changes in SI during 1931–34—2017, recent profile convexity zones (CZ), and SLk indices are overlaid on the anticline axes in Fig. 8.

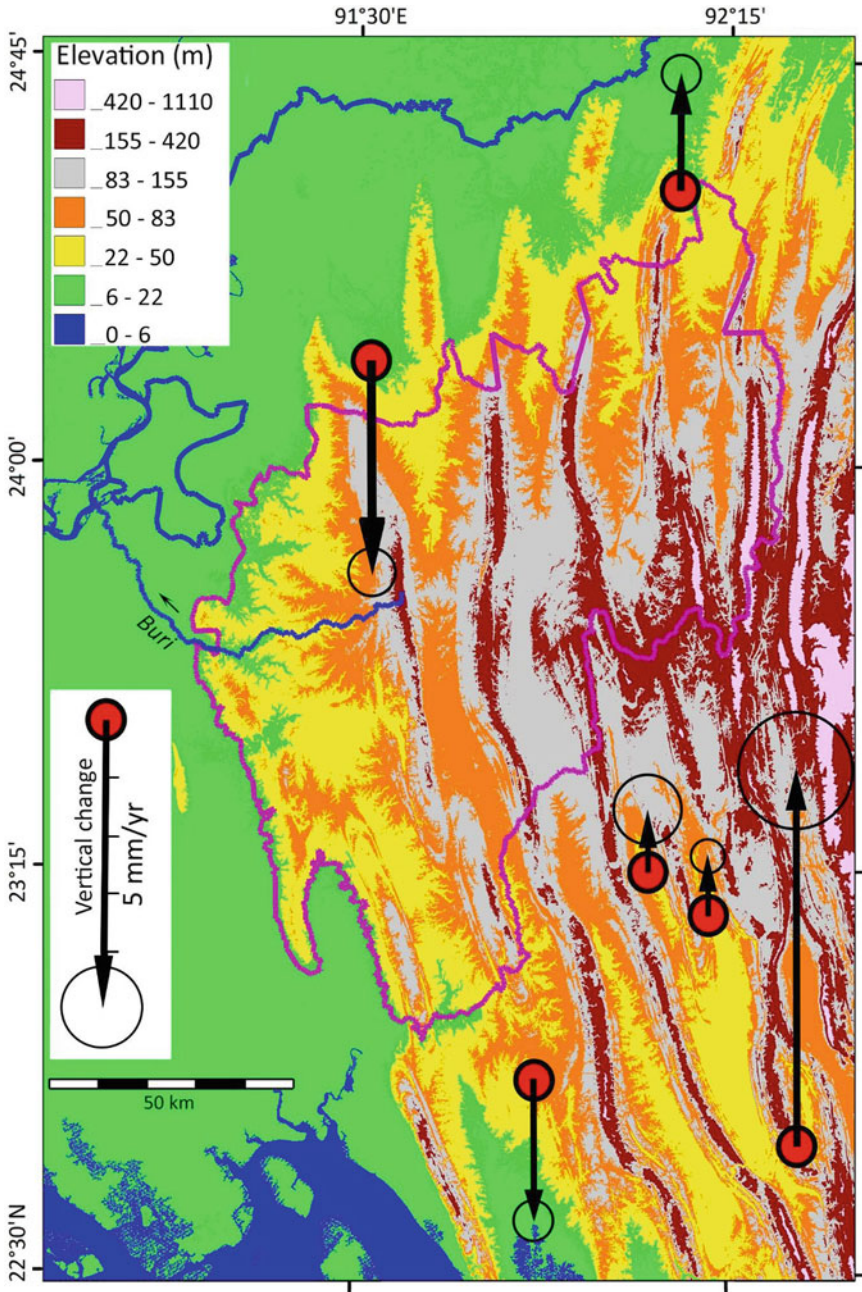


**Fig. 12** Short-term subsidence and uplift rates in CTFB region measured from Global Positioning System observations from 2003/2007 to 2013. Hollow circles around the arrowheads represent  $2\sigma$  uncertainty level. *Source* Elevation model from 2000 SRTM 3 arc second data, vertical change values from Reitz et al. (2015)



The reaches close to the Baramura anticline and the source region of the Buri show low but slightly increasing SI and high SLk values, as can be anticipated in the downstream of an active zone of uplift. The  $\chi$ -map of this region indicates that the divide between the headwaters of the Buri and the Khowai is moving towards the former due to its steeper hydraulic gradient (Fig. 10). The overall alignment of the Buri shows structural control in its reach over the Baramura. It flows parallel to the strike for the first 2.4 km, before turning west. Valley development by differential erosion of soft sediments intercalated between two resistant strata in the western limb of the Baramura anticline was reported before (De and Bandyopadhyay 2011). Similar lineaments are also seen in the Buri Basin, with the course of the Buri deviated at one (greenish dashed line in Fig. 13), and flowing for 2.7 km along the boundary between the Bokabil and Tipam formations (black dashed line in Fig. 13).

The convexity zone-I (CZ-I) is located towards the lower elevations of the Baramura, over sediments accumulated at the slope break. CZ-II coincides with the central anticline, where the reaches display medium SLk indices, but contradictorily, very low to low SI values, all of which have decreased during 1931–34–2017 both in the upstream and downstream portions of the convexity (Figs. 4, 5 and 6). CZ-III and

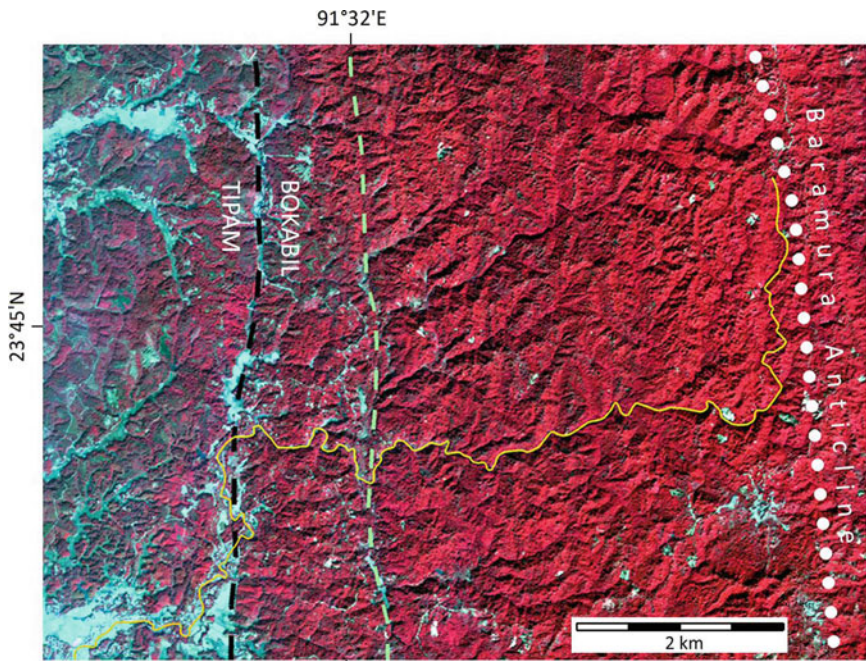


**Fig. 13** Standard False Colour Composite of the Buri's stretch across the western flank of the Baramura range showing structural control. The dotted line denotes anticline axis; light green dashed line, a lineament; black dashed line, the boundary between Bokabil and Tipam formations. See Fig. 3 for location within the Buri basin. *Source* FCC from Resourcesat-2 LISS-4 fmx, Path-110, Row-55, Subscene-D; anticlinal axis and formation boundary from GSI (2011)



CZ-IV are comparatively more subtle, and both are associated with low to medium SI and medium SLk. Similar to CZ-II, the 1931–34—2017 SI also got lowered in CZ-III. In CZ-IV, however, the 1931–34—2017 SI changed positively, following decreasing values of the preceding reaches, as can be expected at a zone of uplift. The relatively lower 2017 SI in the upstream section of CZ-IV compared to its downstream part also connotes possibility of uplift in this region.

Thus, while the observed 2017 SI values and the trends of 1931–34—2017 SI change can be matched with CZ-I and -IV, they do not indicate presence of uplift in CZ-II and -III. This denotes that some local factors like channel modification and/or aggradation may have been responsible for the decrease in the SI in CZ-II and -III between 1931–34 and 2017. This also indicates that the anticlinal axis coinciding with CZ-II is inactive at least for the last ~ 85 yr (Figs. 3 and 8). The general decrease in SI in the zones outside the profile convexities in the Buri's upland section can similarly be related to reduction in gradient due to channel aggradation. It is, however, also plausible that the 90-m resolution of the elevation model was unable pick-up the actual channel altitude because of the Buri's narrow width in these reaches and recorded some portions of the surrounding heights. This may have inaccurately rendered convexity to the channel profile at CZ-II and -III.

On the western edge of its upland section, as the Buri crosses the Rakhia Antiform, SI is low and decreasing, but no profile convexity is detected. This connotes that its vertical erosion completely negated any effect of the anticline's uplift along the channel profile.

Downstream of this region, into the GBMD Plains, the drastic 1931–34—1962 changes in SI was due to channelisation of the Buri to steepen its gradient. This was probably undertaken to improve navigability and/or to make the river more efficient in draining floodwaters from the low-lying farmlands and homesteads of the lower basin. As continuous increase in the post-1962 SI of these reaches suggest, the river is again trying to return to its former equilibrium planform.

As stated earlier, age and elevation of the CTFB's anticlinal ridges decline from east to west (Sect. 2). The Buri seemed to have developed on the western flank of the Baramura as it uplifted and was antecedent to the more western anticlines. The westernmost Lalmai antiform of the CTFB (Fig. 3) is currently buried under the GBMD alluvium and has no surface expression except the Pleistocene residuals appearing at the southern edge of Fig. 3. However, it may have directed the northward orientation of the lower Buri that flows parallel to it, occupying a buried synform. GPS positioning showed that the rates of vertical movement vary throughout the CTFB (Fig. 12). The northward tilting of the Buri Basin, as indicated by its AF (Fig. 9), might be a manifestation of this.

This follows that the lower course of the Buri beyond Nayanpur is inherently younger and more transient in nature than its upland section. This is because, its existence depends on the position of the Meghna or one of its offshoots (e.g., the Titas) within its meander belt. An eastward migration of the Meghna would engulf most of the lower Buri, while westward shift of the Meghna would extend it.

The rainfall records from the north (Agartala) and the south (Udaipur) of the Buri Basin indicated conflicting results of fall at 3.2 mm/yr and rise at 6.2 mm/yr

(Fig. 11). If the trend to the south of the Buri (19.2% of the average rainfall in 71 yr) is considered in view of its low p-value (0.053), it would constitute a proxy of increasing runoff from the region, although with a pronounced yearly fluctuation. Rise in water and sediment discharge is positively related to SI change. Therefore, increase in rainfall cannot explain the decrease in SI along most of the Buri, except in the uppermost reaches. Finally, deforestation and spread of agriculture were not widespread in the Buri Basin during the study period, as seen in other areas of the CTFB; the influence of land use alterations is likely to be negligible on its channel planform.

## 6 Conclusion

The morphometric indices of the Buri—profile convexity, SLk values, AF, and  $\chi$ -map—all indicated presence of active tectonics in the studied part of the CTFB. The river is antecedent to all anticlinal axes along its course. Association of profile convexity, high SLk values, and SI characteristics indicated uplift at the vicinity of the Baramura Range and ~3 km southwest of Bishalgarh. However, decrease in 1931–34—2017 SI and low 2017 SI downstream of the two profile convexity zones were found to be contradictory to expected relationship, and may have been caused either by recent aggradation / modifications of the channel, or by coarse resolution of the elevation model used. The observed SI changes also cannot be linked to rainfall and landuse alterations of the region. In its deltaic stretch, the drastic change in the Buri's SI was caused by channelisation between 1931–34 and 1962.

## References

- Alam M, Alam MM, Curray JR, Chowdhury MLR, Gani MR (2003) An overview of the sedimentary geology of the Bengal Basin in relation to the regional tectonic framework and basin-fill history. *Sed Geol* 155:179–208
- Alam MK, Hasan AKMS, Khan MR, Whitney JW (1990) Geological map of Bangladesh. RF = 1:1,000,000. Geological survey of Bangladesh/United States Geological Survey
- Bandyopadhyay S, De SK (2009) Channel planform change in the northern Chattagram-Tripura Fold Belt, India. Abstracts Volume, 22nd Conference of the Indian Institute of Geomorphologists, University of Allahabad
- Bandyopadhyay S, Saha S, Ghosh K, De SK (2013) Channel planform change and detachment of tributary: a study on the Haora and Katakhal rivers, Tripura, India. *Geomorphology* 193:25–35
- Bandyopadhyay S (2007) Evolution of the Ganga Brahmaputra Delta. *Geograph Rev India* 69(3):235–268
- Beckinsale RP, Chorley RJ (1991) The history of the study of landforms (1896–1950), vol 3. Routledge, London, 496p
- Biswas SK, Agrawal A (1992) Tectonic evolution of the Bengal foreland basin since the Early Pliocene and its implication on the development of the Bengal fan. *Recent Geo-Scientific Studies in the Bay of Bengal and the Andaman Sea. Geolog Surv India Spec Publication* 29:5–19
- Burbank DW, Anderson RS (2012) Tectonic geomorphology. Wiley-Blackwell, Chichester, UK

- Chandra S (2012) Neotectonics and geomorphological regionalisation in India. In: Bandyopadhyay S, Bhattacharji M, Chaudhuri S, Goswami DC, Jog SR, Kar A (eds) *Landforms Processes and Environment Management*. ACB Publications, Kolkata, pp 3–12
- De SK, Bandyopadhyay S (2011) Morphological signatures of fault lines in an earthquake prone zone of southern Baromura hill, north-east India: a multisource approach for spatial data analysis—a critical review. *Environ Earth Sci* 63(2):437–441
- Dey S, Sarkar P, Debbarma C (2009) Morphological signatures of fault lines in an earthquake prone zone of southern Baromura hill, north-east India: a multi sources approach for spatial data analysis. *Environ Earth Sci* 59:353–361
- Friend PF, Sinha R (1993) Braiding and meandering parameters. *Geol Soc Lond Spec Publ* 75:105–111
- Gani MR, Alam MM (2003) Sedimentation and basin-fill history of the Neogene clastic succession exposed in the southeastern fold-belt of the Bengal Basin, Bangladesh: a high-resolution sequence stratigraphic approach. *Sediment Geol* 155:227–270
- Giachetta E, Willett SD (2018) A global dataset of river network geometry. *Sci Data* 5:180127. <https://doi.org/10.1038/sdata.2018.127>
- Goudie A, Viles H (2010) *Landscapes and geomorphology*. Oxford University Press Inc., New York
- GSI: Geological Survey of India (2011) District resource map of West Tripura District, Tripura. RF = 1:250,000
- Hack JT (1973) Stream-profile analysis and stream-gradient index. *J Res US Geol Surv* 1(4):421–429
- Hare PW, Gardner TW (1985) Geomorphic indicators of vertical neotectonism along converging plate margin, Nicoya Peninsula, Coast Rica. In: Morisawa M, Hack TJ (eds) *Tectonic geomorphology. Proceedings of the 15th Annual Binghamton geomorphology Symposium, September 1984*. Allen and Unwin, Boston, pp 123–134
- Holbrook J, Schumm SA (1999) Geomorphic and sedimentary response of rivers to tectonic deformation: a brief review and critique of a tool for recognizing subtle epeirogenic deformation in modern and ancient settings. *Tectonophysics* 305:287–306
- Keller EA, Pinter N (2002) *Active tectonics: earthquakes, uplift, and landscape*. Prentice-Hall Inc., New Jersey
- Kiss T, Blanka V (2012) River channel response to climate- and human-induced hydrological changes: case study on the meandering Hernád river, Hungary. *Geomorphology* 175–176:115–125
- Knighton D (1998) *Fluvial forms and processes: a new perspective*. Arnold, London
- Lawver LA, Scalter JG, Meinke L (1985) Mesozoic and Cenozoic reconstructions of the south Atlantic. *Tectonophysics* 114:233–254
- Maurin T, Rangin C (2009) Structure and kinematics of the Indo-Burmese Wedge: recent and fast growth of the outer wedge. *Tectonics* 28(2):1–21. <https://doi.org/10.1029/2008tc002276>
- McCleary RJ, Hassan MA, Miller D, Moore RD (2011) Spatial organization of process domains in headwater drainage basins of a glaciated foothills region with complex longitudinal profiles. *Water Resour Res* 47:W05505
- Morisawa M (1968) *Streams: their dynamics and morphology*. McGraw-Hill, New York
- Nandy DR (2001) *Geodynamics of Northeastern India and the Adjoining Region*. ACB Publications, Kolkata
- Ntokos D, Lykoudi E, Rondoyanni T (2016) Geomorphic analysis in areas of low-rate neotectonic deformation: South Epirus (Greece) as a case study. *Geomorphology* 263:156–169
- Obruchev VA (1948) Main features of the kinetics and plastics of neotectonics (in Russian). *Izvestiya Akademii Nauk SSSR, Seriya Geologycheskaya* 5:13–24
- Ouchi S (1985) Response of alluvial rivers to slow active tectonic movement. *Geol Soc Am Bull* 96:504–515
- Pedrerá A, Pérez-Peña JV, Galindo-Zaldívar JG, Azañón JM, Azor A (2009) Testing the sensitivity of geomorphic indices in areas of low-rate active folding (eastern Betic Cordillera, Spain). *Geomorphology* 105:218–231

- Pérez-Peña JV, Azañón JM, Azor A, Delgado J, González-Lodeiro F (2009) Spatial analysis of stream power using GIS: SLk anomaly maps. *Earth Surf Process Landforms* 34:16–25
- Persits FM, Wandrey CJ, Milici RC, Manwar A (2001) Digital Geologic and geophysical data of Bangladesh. United States geological survey open-file report 97–470-H. <https://doi.org/10.3133/ofr97470H>
- Reitz DM, Pickering LJ, Goodbred LS, Paola C, Steckler SM, Seeber L, Akhter HS (2015) Effects of tectonic deformation and sea level on river path selection: theory and application to the Ganges-Brahmaputra-Meghna river delta. *J Geophys Res* 120:671–689
- Schumm SA (1963) Sinuosity of alluvial rivers on the Great Plains. *Geol Soc Am Bull* 74(9):1089–1100
- Seeber L, Gornitz V (1983) River profiles along the Himalayan arc as indicators of active tectonics. *Tectonophysics* 92:335–367
- Steckler MS, Mondal DR, Akhter SH, Seeber L, Feng L, Gale J, Hill EM, Howe M (2016) Locked and loading megathrust linked to active subduction beneath the Indo-Burman Ranges. *Nat Geosci* 9:615–618. <https://doi.org/10.1038/NGEO2760>
- Stewart JS (2004). Neotectonics. In: Goudie AS (ed) *Encyclopedia of geomorphology*, vol 1, Routledge, London, p 1156
- Valdiya KS, Sanwal J (2017) Orogenic belt of India–Myanmar border ranges. In: Valdiya KS, Sanwal J (eds) *Neotectonism in the Indian subcontinent: landscape evolution. Developments in Earth Surface Processes*, vol 22. Elsevier, pp 39–150. <https://doi.org/10.1016/B978-0-444-63971-4.00005-0>
- Wang Y, Sieh K, Tun ST, Lai K-Y, Myint T (2014) Active tectonics and earthquake potential of the Myanmar region. *J Geophys Res Solid Earth* 119(4):3767–3822. <https://doi.org/10.1002/2013jb010762>
- Willett SD, McCoy SW, Perron JT, Goren L, Chen CY (2014) Dynamic reorganization of river basins. *Science* 343:1248765